Francisco Vilaplana
Robert G. Gilbert

The University of Queensland, Centre for Nutrition and Food Sciences (CNAFS) and School of Land, Crop and Food Sciences (LCAFS), Brisbane Queensland, Australia

Received July 15, 2010
Revised September 6, 2010
Accepted September 7, 2010

Review Article

Characterization of branched polysaccharides using multiple-detection size separation techniques

The structure of branched polysaccharides involves a hierarchy of levels, from the constituent sugars, then the branching pattern, up to the macromolecular architecture, and then supramolecular organization. Finding causal relations between this complex structure/architecture and both (bio)synthetic mechanisms and final properties is needed for understanding the functionality of branched polysaccharides, which is important in fields ranging from improved nutrition and health through to papermaking and pharmaceuticals. The structural complexity makes this task especially challenging. This review focuses on the best current means to obtain reliable branch chain and size distributions using size-separation technologies coupled with number-, mass- and molecular-weight-sensitive detectors. Problems with current technologies are also critically appraised.

Keywords: Branching / Polysaccharides / Size-exclusion chromatography / Starch
DOI 10.1002/jssc.201000525

1 Introduction

Branched and substituted polysaccharides constitute a structurally heterogeneous family of macromolecules, of great importance in biology, medicine and industrial applications. Different polysaccharides provide structural stability (cellulosic and non-starch polysaccharides), and energy reserves (starches) in biological systems, and they constitute a major energy source for human and animal diets, playing a fundamental role in human nutrition and health. The polysaccharide glycogen is a major glucose buffer (energy storage and supply) in animals and other eukaryotes. In addition to this, polysaccharides constitute the most available renewable resource to mankind for industrial applications, offering the basis for a wide range of polysaccharide derivatives by physical, chemical or enzymatic modification. Structural characterization of such substituted/branched polysaccharides is central for a detailed understanding of the biological and chemical pathways involved during their (bio)synthesis and modification, and for the assessment of their functionality in biological systems and their macroscopic properties in industrial applications. Of particular importance is their degradation during digestion: starch provides 20–50% of food energy for humans, and starch structure is believed to have a significant influence on the rate, including detailed kinetics such as the rates of appearance of polymer degradation products all the way down to glucose; these in turn influence propensity to, and mitigation of, nutritional diseases such as obesity and diabetes. Obtaining such (bio)synthesis–structure–property relations will help reveal currently unknown biological implications and will lead to the optimization of their industrial functionality, as well as to foods and food processing with improved nutritional properties.

The chemical structure of branched/substituted polysaccharides can be hierarchically described over different levels of organization (Fig. 1). The first structural level corresponds to the nature of the monomers (sugars) that constitute the polysaccharide, whether homo- or co-polymer. The second level of structure is related to the substitution/branching pattern of the polysaccharide, which depends on the distribution of the covalent linkages along the constituent sugars. This leads to a wide range of possible architectures in the whole polysaccharide macromolecule (third level of structure): from completely linear polysaccharides (cellulose), linear polymers with alternating bonds (β-glucans), substituted polysaccharides with linear backbones (arabinoxylans), synthetically modified poly-

Correspondence: Dr. Robert G. Gilbert, Centre for Nutrition and Food Sciences (CNAFS) and School of Land, Crop and Food Sciences (LCAFS), The University of Queensland, Hartley Teakle Building, Brisbane Queensland 4072, Australia
E-mail: b.gilbert@uq.edu.au
Fax: + 61-7-33651188

Abbreviations: DRI, differential refractive index; **FACE,** fluorophore-assisted CE; **FFF,** field flow fractionation; **HDC,** hydrodynamic chromatography; **FACE,** fluorophore-assisted CE; **MALLS,** multi-angle laser light scattering; **MTF,** molecular-topology fractionation; **MW,** molecular weight; **PAD,** pulsed amperometric detection; **QELS,** quasi-elastic light scattering; **SEC,** size-exclusion chromatography; **TGIC,** temperature-gradient interaction chromatography

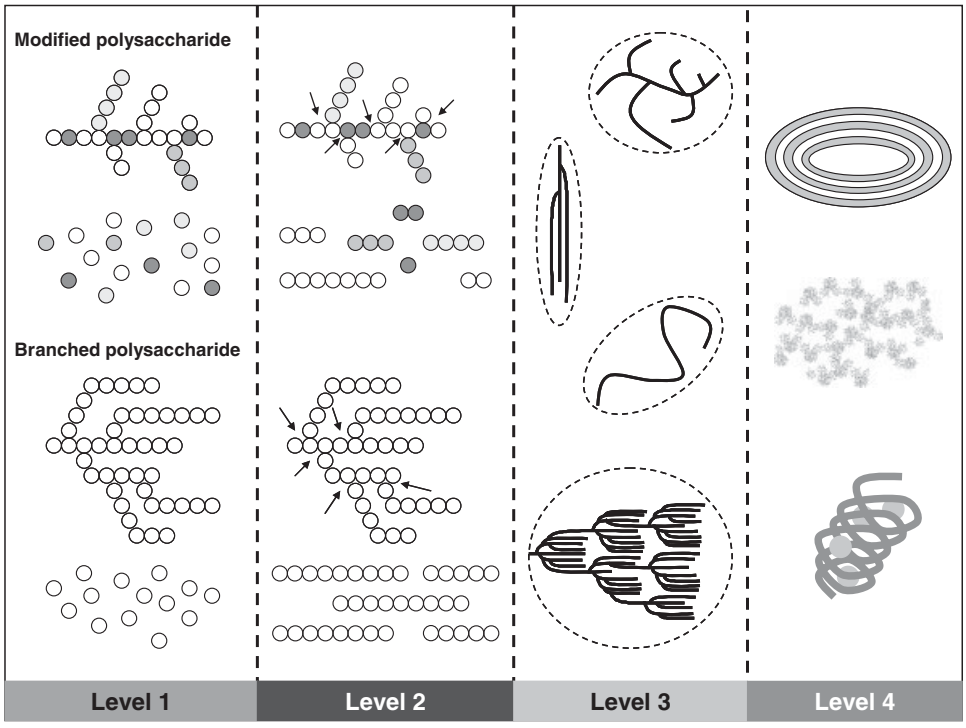

Figure 1. Structure levels in modified/branched polysaccharides: Level 1 (constituent monomeric sugars); Level 2 (substitution/branching pattern of the polysaccharide and its branch chain-length distribution); Level 3 (whole polysaccharide macromolecule); and Level 4 (supramolecular organizations).

saccharides through grafting (cellulose and starch derivatives), to more complex fully branched polysaccharides with random or predetermined branching structures such as the glucose homopolymers glycogen and starch. Starch in turn comprises amylose, of relatively low molecular weight (MW) with a few long-chain branches, and amylopectin, of very high MW and with many short branches. Such macromolecular architectures may arrange themselves in further supramolecular organizations (Level 4), with intra- and intermolecular interactions and/or with interactions with other compounds present in the biological system or industrial product, which in the end determine their activity and properties in the desired applications.

The analysis of the constituent monomeric sugars is a well-established process combining acid hydrolysis, derivatization, and finally separation and quantitative evaluation by chromatographic or electrophoretic techniques [1, 2]. Taking into account the second structural level, different approaches can be followed to evaluate the substitution/branching pattern in branched polysaccharides. NMR spectroscopy (both 1-D and 2-D) provides data on the degree of substitution and/or degree of branching at a monomeric level [1–4]. For further details on the substitution/branching distribution within the polysaccharide molecule, more selective approaches must be taken, by performing partial hydrolysis of the polysaccharide and subsequent analysis of the products. Partial hydrolysis can be performed either randomly (by acid hydrolysis, for example) or preferably by enzymatic treatment (amylases, amyloglucosidase, glucosidase, pullulanase and isoamylase) to cleave specific linkages along the polysaccharide chain [4]. Further analysis of the resulting fragments can be performed by CE (after quantitative labelling), chromatographic techniques (*e.g.* size-exclusion chromatography (SEC)) or by soft ionization mass spectrometric techniques such as ESI or MALDI [2, 4, 5]. The structural analysis of the whole substituted/branched macromolecule is usually performed by size-separation technologies coupled with different detectors, to yield meaningful size distributions (mass, number and MW) that describe the individual macromolecular structural features. This structural level largely controls the higher organizational levels and the functionality and properties of the polysaccharides. There are no methods as yet to fully characterize this last level of structure, and much work is still to be done to achieve such goal. A fundamental part of this review will be devoted to describe the state-of-the-art of the technology related to this level of structure and its current challenges and limitations.

The structural characterization of branched polysaccharides at a macromolecular level is a challenging task, due to their complex architecture. Just considering the case of a branched polysaccharide with the same repetitive monomeric sugar constituent (*e.g.* α-D-glucopyranosyl for starch or glycogen), an infinite-dimensional distribution is required for its unambiguous comprehensive structural characterization, considering the individual size of the branches (the chain-length distribution), the number of branches, and the position of a given branch of a given DP from the nearest branch of another given DP … *ad infinitum* (Fig. 2) [6]. This infinite-dimensional distribution is intractable in practice, but gives the theoretical basis for predicting a wide range of experimental observables from size-separation techniques coupled with multiple detection. These observables include average values such as average

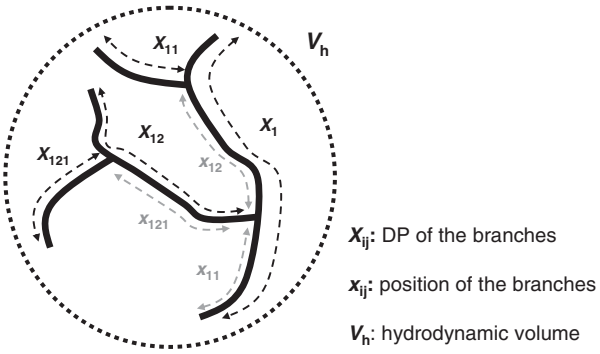

Figure 2. General description of the structure of a branched polysaccharide. Redrawn from the schematic given in [6].

size and MW, 1-D structural distributions based on macromolecular size (*e.g.* the hydrodynamic radius or radius of gyration, depending on the technique used for determination), 1-D chain-length distributions of the branches, and 2-D distributions based on size/branching. Sample preparation also constitutes a fundamental issue in obtaining reliable structural information [7].

The purpose of this review is to describe the currently available size-separation technology to obtain size distributions applicable for the elucidation of the macromolecular structure of branched polysaccharides, including the chain-length distributions of the individual branches. Special emphasis will be given to natural branched polysaccharides such as starch and glycogen, due to their biological, medical and industrial importance. The results can in most of the cases be extended to other natural and synthetic branched and modified polysaccharide-based materials, including starch and cellulose derivatives. Traditionally, empirical correlations have been employed to link (bio)synthetic mechanisms and desired target properties; average MWs have been also employed for industrial purposes to assess molecular structure with final macroscopic properties. Size distributions offer substantially more information about the complex structure of branched/modified polysaccharides and are fundamental to elucidate the correlations between (bio)synthesis, structure and properties, which will result in improved (bio)synthesis, target properties and final applications.

2 Sample preparation requirements

Sample preparation involves all the preparative steps that are required to extract the branched polysaccharide from its original source and to prepare the sample in a suitable form for size separation and detection. Depending on the material and purpose of the investigation, sample preparation can be as simple as dissolving the given polysaccharide in a suitable solvent for separation (if a commercial sample or an industrial product is employed) or much more elaborate procedures involving a number of consecutive steps to isolate the compound from the original natural source, subsequent purification and final dissolution. The optimal sample preparation requirements for a successful size separation of the target branched polysaccharide are:

(i) Achieving complete molecular dissolution of the polysaccharide, preferably in the same solvent system that will be employed for size separation, avoiding the formation of supramolecular aggregates that will bias the results from size determinations.
(ii) Preventing molecular degradation of the polysaccharide during each step of the sample preparation protocol. Polysaccharides are especially sensitive to degradation processes through chemical, thermal, biological or mechanical degradation, so special precautions must be considered when designing the experimental procedure.
(iii) Removing all existing non-polysaccharide impurities that may affect the separation and the determination of the structural size distributions.
(iv) Preventing any sample loss during each step of the procedure, or at least any sample loss that may be biased to any of the structural parameters, such as size or branching density.

Native polysaccharides are very difficult to dissolve without degradation, due to strong hydrogen bonding between the hydroxyl groups. Traditionally, branched polysaccharides have been pretreated using relatively harsh conditions (heating at elevated temperatures, microwave irradiation, sonication, mechanical stirring, high-pressure treatments and use of alkaline solutions) (*e.g.* [8–11]), but these procedures may induce molecular degradation and thus lead to inaccurate results with regard to their size distributions [7, 12]. It has been demonstrated that DMSO, sometimes together with lithium salts as hydrogen-bond disrupter at moderate temperatures (below 100°C), completely dissolves starch without significant degradation [13]. This solvent system also prevents the polysaccharide adsorption onto the stationary phases typically employed in size separations (namely, SEC) and contributes to avoid the formation of supramolecular aggregates and retrogradation [7]. Commercial, processed and modified branched polysaccharides are usually much easier to dissolve than their native counterparts, precisely due to all the previous steps that have led to such products and that may have induced molecular degradation to facilitate their posterior handling.

A successful protocol for the extraction, purification and dissolution of starch from cereal grains has been recently proposed [12]. This procedure involves multiple steps, including mild cryogenic grinding to release starch granules from the original grains, protease treatment to hydrolyse protein contaminations, dissolution in DMSO containing LiBr to dissolve starch granules, starch precipitation with ethanol and centrifugation to remove non-starch materials (lipids, protein fragments and non-starch polysaccharides), and final dissolution in the desired solvent for size separation. While this protocol follows well-established procedures for cereal

grain treatments and starch extraction and dissolution, these procedures have not hitherto been implemented systematically for this purpose. Similarly, a procedure for the purification of glycogen from mammalian liver tissue has been recently developed [14], which maintains the structural and morphological features of native glycogen unaltered.

3 Size distributions from multiple detectors after size separation

Structural information for branched polysaccharides is usually obtained from size-separation techniques, such as SEC or field-flow fractionation (FFF), coupled with multiple detector systems (usually number-, mass- and MW-sensitive detectors). As stated, the complete description of the structure of a complex branched polymer requires an infinite-dimensional distribution function. The individual application of these various experimental techniques offers different 1-D views of the infinite-dimensional one, depending on the nature of the detector employed.

For linear homopolymers (linear or quantitatively debranched polysaccharides in the case of this review), there is a unique relation between the size-separation parameter (termed the hydrodynamic volume, V_h, the definition of which [15] depends on the technique employed) and the MW M, or the DP X. These last quantities are, for glucose homopolymers, related by $M = 162.2X + 18.0$, 162.2 being the molar mass of the monomeric unit and 18.0 that of the additional water in the end groups. The relation between M and V_h is obtained by some sort of calibration procedure, usually universal calibration (in the case of SEC) or using detectors such as light scattering that are MW-sensitive. Size separation of linear polymers under ideal conditions (this is, in the absence of band broadening) will provide a completely monodisperse polymer sample (dispersity $Đ = \{\bar{M}_w/\bar{M}_n\} = 1$) for each slice of elution volume (V_{el}). Hence size separation coupled with a single mass-, number-, or MW-detector is usually sufficient to provide complete structural characterization of the molar mass distribution for a linear homopolymer. This information can be presented equivalently in terms of the number distribution $N_{de}(X)$ of chains of DP X, or the weight distribution $W_{de}(X)$ of chains of DP X, or the so-called SEC distribution $w_{de}(\log X)$, which is the theoretical distribution obtained from SEC in ideal conditions [16] (in the absence of band broadening and where a log-linear relation is observed between M and V_{el}). These distributions are trivially related for linear polymers using the following equation:

$$w_{de}(\log X) = X\ W_{de}(X) = X^2\ N_{de}(X) \quad (1)$$

In the case of branched polymers, there is no longer a direct relation between the separation parameter (V_h) and the MW. The size distributions must be then always presented in terms of some size parameter. This parameter can be the hydrodynamic volume V_h, or equivalently the hydrodynamic radius, R_h, with $V_h = 4/3\pi\ R_h^3$, or the radius of gyration R_g, if available. Other possibilities are the MW of a standard (*e.g.* polystyrene) that has the same hydrodynamic volume as the analyte: an 'equivalent MW'; however, this is not recommended because it can convey the impression that this is a true MW, when that is certainly not the case. Size distributions of a branched polymer must never be given solely in terms of elution time or elution volume, since these are dependent on the instrumental conditions and may vary from day-to-day and from run-to-run. Alas, this incorrect practice is not uncommon, despite the fact that such a form of data presentation breaks an essential requirement in presenting scientific data, inasmuch as it is not reproducible. Some sort of calibration must be therefore performed to convert the experimental elution times or volumes into an appropriate molecular size. For a complex branched molecule, at each slice of V_{el} corresponding with a certain hydrodynamic volume, there is no longer a monodisperse polymeric sample but a distribution of molecules with different branching structures and MWs, where the dispersity $Đ$ at that V_h is no longer unity and $\bar{M}_W \neq \bar{M}_n$. The size distributions are therefore no longer trivially related by Eq. (1) (or some equivalent), and different detectors are needed to obtain correspondingly the number distribution, $N(V_h)$, the SEC weight distribution, $w(\log V_h)$, the size dependence of weight-average MW, $\bar{M}_W(V_h)$, and the size dependence of the number-average MW, $\bar{M}_n(V_h)$. It is noted that the normalization of distributions, such as $N(V_h)$, $W(V_h)$ and $w(\log V_h)$, is arbitrary, and so there is no normalization specified in the relations between these quantities and detector signal. However, quantities such as $\bar{M}_W(V_h)$ have no such arbitrary normalization (they are absolute numbers) and so it is essential to fully specify quantities and units relating these to detector signal. This section will update and correct relations given in previous work [17] for the size distributions for branched polymers (and polysaccharides in particular) and for the way they can be calculated using various postseparation detectors.

The differential refractive index (DRI) detector is a concentration-sensitive detector widely employed for the characterization of polymers, which measures the difference in refractive index between the pure solvent in a reference cell and the solution containing the sample, in a different cell. The signal of the DRI is dependent on an instrumental factor f_{DRI}, the concentration at each elution volume, $c(V_{el})$, and a sample-dependent parameter, the refractive index increment dn/dc (where n is the refractive index), which depends on the type of polysaccharide, the solvent, the wavelength and the temperature

$$S_{DRI}(V_{el}) = f_{DRI}\ dn/dc\ c(V_{el}) \quad (2)$$

The DRI detector gives directly the SEC weight distribution through Eq. (3) [17], where $S_{DRI}(V_{el})$ is the DRI signal and $\tilde{V}_{el}(V_h)$ is the universal calibration curve giving the dependence of elution volume on hydrodynamic volume

$$w(\log\ V_h) = -S_{DRI}(V_{el})\frac{d\tilde{V}_{el}(V_h)}{d\ \log\ V_h} \quad (3)$$

The number distribution $N(V_h)$ can be directly obtained after size separation using a number-sensitive detector, such as fluorescence or UV, if quantitative labelling of each branched polysaccharide is performed independently of macromolecular size, *e.g.* if exactly one chromophore or fluorophore is attached individually to the reducing end of each polysaccharide molecule. However, it has not been established if any such labelling procedures are quantitatively valid for large branched polysaccharides. Indeed, it is hard to envisage a way that this could be proved for complex branched polymers, apart from comparison with the unlabeled parent distributions, which are the object of the labelling. Hence, any distributions obtained could be biased in any or all of size, branching structure and MW and so would not be reliable. It is however noted that this has been proven successful for labelling debranched starch [18].

An indirect approach to calculate the number distribution is through the viscometric detector, which measures the pressure differences in different capillary tubes containing either the pure solvent or the sample solution. The specific viscosity (η_{sp}) is directly calculated from these pressure differences along the viscometer, and it offers a means of finding the number distribution using the following equation [6]:

$$N(V_h) = -\frac{\eta_{sp}(V_{el})}{V_h^2}\frac{d\,\tilde{V}_{el}(V_h)}{d\log V_h} \quad (4)$$

The viscometer in conjunction with the refractometer provides means of calculating the intrinsic viscosity [η], which is an important property of the polysaccharide in solution. This calculation can be performed considering that, after size separation, the samples are very diluted (and therefore concentration tends to zero). The size dependence of the number-average MW $\bar{M}_n$ can be calculated from the intrinsic viscosity using the definition of hydrodynamic volume derived from the Stokes–Einstein relation (Eq. 6):

$$[\eta](V_{el}) = \lim\,(c \to 0)\frac{\eta_{sp}(V_{el})}{c(V_{el})} \quad (5)$$

$$\tilde{M}_n(V_h) = \frac{5}{2}\frac{V_h\,N_A}{[\eta]} \quad (6)$$

where N_A is Avogadro's constant and the intrinsic viscosity [η] is that in the increment of elution volume; note that Eq. (6) contains the correct form of V_h for SEC separation, because it is this form for which there is experimental evidence that this V_h is the size-separation parameter [19–21].

The size dependences of the weight-average MW, $\bar{M}_w(V_h)$, and of the root-mean-square *z*-average radius, the mean radius of gyration $\bar{R}_g(V_h)$, can be obtained from combined multi-angle laser light scattering (MALLS) and concentration detectors (usually DRI for polysaccharides). Light scattering provides absolute weight-average MW and average macromolecular size ($\bar{R}_g$) in solution, given values of appropriate quantities such as d*n*/d*c*. The root-mean-square *z*-average radius ($R_{g,z}$) is independent of the refractive index increment d*n*/d*c;* however, other statistical moments of R_g are not. The intensity of the light scattered by a monodisperse macromolecule is dependent on both concentration and MW. For very dilute macromolecular systems in solutions, a condition which is expected to be valid for size separations, the excess Rayleigh ratio of scattered light at a certain angle θ *versus* the incident intensity (R_θ) can be expressed following the well-known Zimm equation (Eq. 7) [22] (for detailed information about the mathematical treatment of light scattering data for macromolecular characterization, reviews from Berry, Burchard and Wyatt [23–26] are recommended). *K* in Eq. (7) is a physical constant dependent on the refractive index of the solvent (n_0), the vacuum wavelength of the incident light (λ_0) and d*n*/d*c*; A_2 is the second virial coefficient; and $P(\theta)$ is the scattering function that describes the angular variation of scattered light

$$R_\theta(V_{el}) = K\,c(V_{el})\,[P(\theta)\bar{M}_W(V_{el}) - 2\,A_2\,\bar{M}_W^2(V_{el})\,P^2(\theta)\,c(V_{el}) + \cdots] \quad (7)$$

$$K = \frac{4\,\pi^2(dn/dc)^2\,n_0^2}{N_A\,\lambda_0^4} \quad (8)$$

The scattering function $P(\theta)$ depends on the relative distances of the scattering points within the macromolecule and can be related to $\bar{R}_g$. Different expressions have been proposed to describe $P(\theta)$, depending on the macromolecular conformation and its size. From its definition, it is known that in the limit when the scattered angle θ tends to 0, then $P(\theta) = 1$. The most common procedures to extrapolate to $\theta = 0$ are those of Zimm [27], Debye [28] and Berry [29], which are basically different methods of plotting the angular dependence of the light scattering data. Fitting SEC-MALLS-DRI data assumes infinitely dilute concentrations in each slice of elution volume, so modified Zimm, Debye and Berry methods can be used to evaluate the values of the weight-average MW and the radius of gyration at each slice of elution volume. In modified Debye plots (Eq. 9), $R_\theta(V_{el})/(K\,c(V_{el}))$ is plotted *versus* $\sin^2(\theta/2)$, while modified Berry plots (Eq. 10) use the square root of the quantities used in Debye plots. Note that λ refers to the wavelength of the incident light in the separation medium (Eqs. 9 and 10), in contraposition with the vacuum wavelength of the incident light (λ_0) in Eq. (8). The values of $\bar{M}_W$ for each slice of elution volume are calculated from the intercept of the plotted values at 0° (and thus the size dependences of the weight-average MW, $\bar{M}_W(V_h)$, can be obtained), and the $\bar{R}_g$ values are calculated from the slope when the angle tends to 0°

$$\frac{K\,c(V_{el})}{R_\theta(V_{el})} = \frac{1}{\bar{M}_W(V_{el})} + \frac{16\,\pi^2}{3\,\lambda}\frac{1}{\bar{M}_W(V_{el})}\bar{R}_g^2(V_{el})\sin^2\left(\frac{\theta}{2}\right) \quad (9)$$

$$\sqrt{\frac{K\,c(V_{el})}{R_\theta(V_{el})}} = \sqrt{\frac{1}{\bar{M}_W(V_{el})} + \frac{16\,\pi^2}{3\,\lambda}\frac{1}{\bar{M}_W(V_{el})}\bar{R}_g^2(V_{el})\sin^2\left(\frac{\theta}{2}\right)} \quad (10)$$

A study by Andersson *et al.* [30] showed that the accuracy of $\bar{M}_W$ and $\bar{R}_g$ can vary substantially depending on the extrapolation method, especially for larger macromolecules (>100 nm), where the extrapolation errors can become large. Care must be then taken when analysing MALLS data for branched polysaccharides, especially for the larger ones (*e.g.* amylopectin). For smaller polysaccharides, the Zimm and Berry methods generally offer accurate results. However, advanced extrapolation methods, perhaps taking into account more complex dependencies and higher order terms for the scattering function $P(\theta)$ [31–33], may be needed to obtain reliable absolute $\bar{M}_W$ and $\bar{R}_g$ values for amylopectin, the large hyperbranched type of starch. The routine implementation of such procedures in commercial software is worthy of consideration.

Light scattering also offers a robust procedure to assess the conformation of macromolecules in solution, the so-called fractal dimension [34], by performing conformational plots of $\bar{R}_g$ *versus* $\bar{M}_W$. For polymers with dispersity close to unity, this dependence is well described by a simple power expression (Eq. 11), referred to as the de Gennes scaling law concept [35]:

$$\bar{R}_g = K_g(\bar{M}_W)^{\nu_g} \quad (11)$$

Here K_g is a constant depending on monomer structure and the nature of the solvent, and the exponent ν_g depends on the polymer architecture, temperature and polymer–solvent interactions ($\nu_g = 0.5$–0.6 corresponds to a linear random coil conformation in solution, $\nu_g = 0.33$ to a hard sphere of homogeneous density, and $\nu_g = 1$ to a rigid rod of homogeneous density). The scaling law behaviour seems to be followed well for linear and slightly substituted polysaccharides [36, 37], whereas for complex branched polysaccharides such as glycogen or amylopectin, deviations from this power scale law have been reported [38].

4 Size-separation technology for structural analysis of branched polysaccharides

The implementation of successful size-separation technologies is fundamental for obtaining reliable size distributions and thus for the structural characterization of substituted and branched polysaccharides. Different techniques can be applied for both the characterization of the full-branched macromolecular size (Level 3) and the chain-length distribution (size) of the branches (Level 2). The difference is the separation resolution that is required for the wide range of sizes of the different polysaccharide systems. The goal of any analytical procedure (here, size separation of branched polysaccharides) is to provide information applicable to certain goals, usually obtaining (bio)synthesis–structure–property relations, and also quality assurance for industrial processes. Achieving good separation is fundamental to these goals, and it always must be borne in mind that the characterization data need to be appropriate in type and accuracy for the desired goal: for example, the demands for structural data for quality assurance may be much less than for elucidating certain types of structure–property relations.

The main prerequisites for a successful size separation are:

(i) To have a representative amount of fully dissolved sample, preferably in the mobile phase solvent system, without contamination and without degradation induced by sample preparation. These issues were addressed in the sample preparation part of the discussion.
(ii) To perform any derivatization or labelling steps required for optimized detection, with the need for a quantitative response, so meaningful distributions without any biasing can be obtained.
(iii) To completely inject a sufficient amount of sample to be detected after separation, without overloading the system or causing particle aggregation, degradation or causing a decrease in the resolution separation.
(iv) To achieve optimized separation resolution during the elution step with regards to size, providing a reliable and stable response in the detection step. Some technologies can provide baseline-resolved individual peaks, as is the case of CE for linear oligosaccharides up to $X \sim 80$ (*e.g.* the short branches of amylopectin and glycogen); some other techniques must deal with the problem of band broadening (this is, co-elution of multiple sizes at the same elution volume). These issues will be discussed below.
(v) To provide separated sample amounts for the detectors to provide an adequate S/N, without overloading the detectors, so reliable size distributions can be then calculated from the detector response.
(vi) To obtain data that are well-defined molecular quantities (*e.g.* weight of molecules as a function of molecular size), rather than machine-dependent ones (such as weight of molecules as a function of elution volume), and that are thus reproducible.

4.1 Separation techniques for obtaining the chain-length distributions of linear (debranched) polysaccharides

Fluorophore-assisted CE (FACE) is currently the best technique for the chain-length analysis of maltooligosaccharides, offering individual chain-length baseline resolution for each X up to $X \sim 85$, and therefore ideal for the analysis of the short branches of amylopectin and glycogen (after enzymatic debranching of the whole molecule) [18, 39]. The experimental procedure consists of labelling the reducing end of the linear maltooligosaccharide with a fluorophore (typically 8-amino-1,3,6-pyrenetrisulfonic acid) and performing the separation using CE with fluorescence detection. Quantitative labelling of the linear oligosaccharides with 8-amino-1,3,6-pyrenetrisulfonic acid has been

proven to be size independent up to $X \sim 135$ [18]; other labelling procedures are being currently explored with higher sensitivity, milder synthetic conditions and expanded applicability in terms of polysaccharide chain length (for a state-of-the-art review on labelling of carbohydrates for CE applications, refer to [40]). High-performance anion-exchange chromatography at high pH with pulsed amperometric detection (HPAEC-PAD) can also be employed for the analysis of oligosaccharides from debranched amylopectin and glycogen with baseline resolution up to $X \sim 80$ [41, 42]. However, the response of the amperometric detection seems to depend on the chain length of the polysaccharide, so the resulting chain-length distributions may be biased unless they are corrected by using response factors [43]. MALDI-ToF-MS could potentially offer the MW distributions of linear (debranched) polysaccharides, but mass discrimination effects at high MWs may introduce artefacts in the resulting distributions. For example, Broberg *et al.* compared the chain-length distributions for debranched amylopectin obtained from HPAEC-PAD and MALDI-TOF, and showed that the latter overestimated the amount of the longer chain units [44].

The analysis of the chain-length distributions of debranched polysaccharides (Level 2 of structure) is fundamental for understanding the higher level macromolecular architectures of the branched molecules, and appropriate correlations with (bio)synthetic pathways and the properties and functionality in biological systems. The distributions of debranched chains obtained from FACE or HPAEC-PAD are the debranched number distribution $N_{de}(X)$ and the weight distribution $W_{de}(X)$, respectively. These are related by $W_{de}(X) = X\, N_{de}(X)$, and can be directly applied to obtain mechanistic information about the biosynthetic pathways of starch and glycogen molecules. These are traditionally represented as frequency plots, *i.e.* $N_{de}(X)$ normalized so that the sum of $N_{de}(X)$ over all DPs X is 1, or as difference plots, which are the differences between a series of such normalized $N_{de}(X)$ compared to some reference distribution (*e.g.* mutant varieties compared to the wild type). Castro *et al.* [45] introduced a new way of plotting the chain-length distributions for debranched polysaccharides, $\ln N_{de}(X)$ as a function of X, which clearly identifies different regions in the branch distribution of amylopectin and glycogen, and brings out significant features for higher DPs that are not apparent in simple frequency or difference plots at higher X. Comparing different $\ln N_{de}(X)$ also eliminates any artefacts due to normalization (comparing two $N_{de}(X)$ summed to unity will be biased if they cover different ranges of X). Further application of these $\ln N_{de}(X)$ plots from FACE reveals genetic diversity in starch amylopectin samples arising from slight differences in (bio)synthesis with, for example, mutations, which affects macroscopic properties [46]. This is exemplified in Fig. 3.

At present there is no universal technique that offers fully resolved chain-length distributions of debranched starch for both the amylopectin and amylose populations. Both FACE and HPAEC-PAD are constrained by the upper chain-length limit, and therefore neither the debranched distribution of amylose nor longer amylopectin chains can be obtained from these techniques. SEC is at present the best technique to use for a comprehensive characterization and comparison of the entire range of debranched chain-length distributions, taking into account that individual chain-length distributions (resolution of individual DPs) cannot be obtained due to separation limitations (*i.e.* insufficient chromatographic resolution and band broadening). A procedure for taking into account band broadening in the debranched chain-length distributions for starch (or any linear or quantitatively debranched polysaccharide) obtained from SEC was presented by Castro *et al.* [47]; this was implemented by the deconvolution of the ''broadened'' raw data from DRI and MALLS detection after SEC separation, compared to the true chain-length distribution obtained from FACE as a reference. This deconvolution procedure reveals structural features in the chain-length distribution, such as shoulders, which were qualitatively hidden in the SEC profiles due to band broadening and poor separation resolution. A method of correcting for band broadening that is suitable for the higher DPs where FACE data are unobtainable has been developed [48, 49].

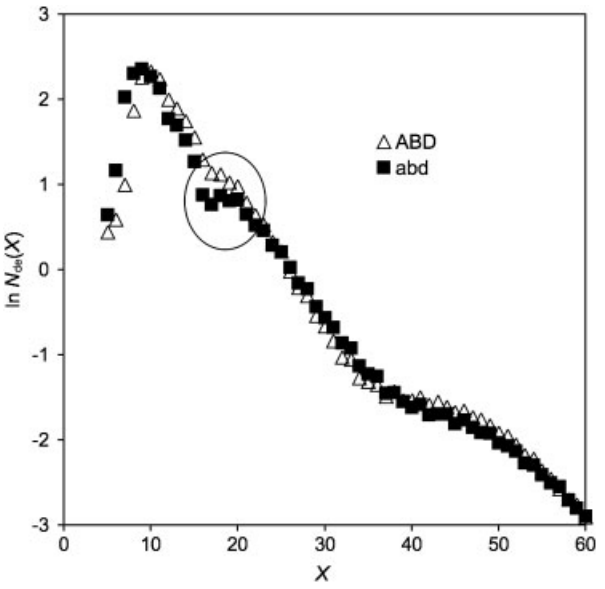

Figure 3. Chain-length distributions for wheat, as ln $N_{de}(X)$ for a wild-type (ABD = wild-type) and mutant (abd = null-type). Data replotted from data in Fig. 4 in [46]. The region showing significant differences arising from the genetics of the mutation is circled.

4.2 Separation techniques for obtaining the size distributions of branched polysaccharides

The size separation of substituted and branched polysaccharides (Level 3 structure) for structural characterization is through LC (SEC) and FFF. The applicability, advantages and limitations of these techniques for branched poly-

saccharides will be discussed in this section, together with some recent results obtained by our group as an example of their applicability to obtain size distributions and unveil (bio)synthesis–structure–property relations.

4.2.1 SEC

SEC (often called gel-permeation chromatography) coupled with multiple detection is, currently, the most readily available and most developed technology for the size separation of branched polysaccharides and thus obtaining their size distributions. SEC separates macromolecules in solution by their size or hydrodynamic volume (V_h), which for SEC is proportional to the product of the weight-average intrinsic viscosity $[\bar{\eta}_W]$ and the number-average MW $\bar{M}_n$ [19–21] (see Eq. 6 for the proper derivation of this V_h). Size separation is achieved throughout the equilibrium established between the mobile phase when it is stagnant in the stationary-phase pores and when it is eluting; smaller molecules will be retained longer in the pores than larger ones and will elute later. The analytes should not interact enthalpically with the stationary phase in order to achieve the proper size-separation regime.

SEC is well established for the separation of polysaccharides, with reliable instrumentation and a wide range of commercially available stationary phases over a broad range of macromolecular sizes, compatible with the common solvent systems used for polysaccharides. These solvent systems are typically water-based or polar aprotic solvents, such as DMSO or dimethyl acetamide, to which may be added hydrogen bonding disrupting salts, such as LiBr or LiCl. The separation range of SEC technology covers oligosaccharide molecules up to polysaccharides, depending on the pore exclusion limit of the commercially available stationary phases (the separation resolution of larger macromolecules is poor in the range of the exclusion limit). Indeed, high molar mass separations of native starches have been reported by SEC with large-pore packing materials [50]. Materials with pores over 100 nm are commercially available; this value is in the range of the upper limit of calibration of current ''monodisperse'' standards used for calibrating the system. Larger molecules, such as amylopectin or modified polysaccharide derivatives, can still be characterized using SEC, but several limitations arise in this application.

4.2.1.1 Size calibration

Size calibration of SEC for polysaccharide analysis is usually performed using a series of narrow-dispersity linear glucan standards (pullulan or dextran) of known $\bar{M}_n$ to give the relation between elution volume and hydrodynamic volume, $\tilde{V}_{el}(V_h)$, through the 'universal calibration' principle. This is the assumption that SEC separation of any polymer is only by its hydrodynamic volume, irrespective of its structure, size and composition. V_h for size separation by SEC is given by:

$$V_h = \frac{2\,[\bar{\eta}]_w(V_h)\,\bar{M}_n(V_h)}{5\,N_A} \tag{12}$$

where $[\bar{\eta}]_w(V_h)$ and $\bar{M}_n(V_h)$ are respectively the weight-average intrinsic viscosity, and number-average MW, of polymer with hydrodynamic volume V_h. That separation in SEC depends only on V_h and not on any structural parameters has been postulated based on limited experimental data for branched polymers (including starch) [19, 20, 51]. This widely adopted assumption merits further experimental checks for polysaccharides with a range of structures and solvents, as it may well not be valid for some (or even many) such analytes.

The experimental determination of V_h for the set of moderately monodisperse linear standards with known $\bar{M}_n$ can be done using combined viscometric and DRI detection using the following equation:

$$V_h = \frac{2}{5}\frac{M_n\,[\eta]}{N_A} \tag{13}$$

When viscometric detection is unavailable and thus the experimental universal calibration cannot be implemented, the calibration curve can still be performed if the Mark–Houwink parameters K and α are known for the calibration standards (pullulans/dextrans) in the solvent system and the temperature of separation (Eq. 14). It is noted that the empirical Mark–Houwink relation is only valid for a limited range of M for linear polymers (usually it deviates for M below $\sim$1000 Da and above $\sim 10^6$ Da) and, although widely used, may not be valid for particular calibrants, so universal calibration with experimental measurement of the intrinsic viscosity is preferred when available

$$V_h = \frac{2}{5}\frac{K\,M_n^{1+\alpha}}{N_A} \tag{14}$$

As mentioned earlier, one of the limitations of SEC is the restricted range of sizes in which universal calibration can be performed, due to the lack of commercially available standards. The calibration range covered is applicable for polysaccharides ranging from simple sugars to linear polysaccharides in the range of $M \sim 10^6$ Da (corresponding to a macromolecular size up to $R_h \sim 50$ nm); this calibration range covers medium-sized polysaccharides such as β-glucans, arabinoxylans, amyloses and glycogen, but not larger molecules as amylopectin. Even if larger standards existed, additional problems may occur such as poor separation resolution for such sizes (from the exclusion limit of the stationary phase pores) and the occurrence of shear scission during elution. Extrapolation of the available calibration curves to larger volumes is possible and usually performed, but the results thus obtained are only qualitative. Indeed, extrapolation of the calibration curve for large molecules is very sensitive to the slight changes in elution behaviour in these size ranges (including day-to-day variation), which normally fall beyond the exclusion limit for SEC and therefore behave in the hydrodynamic chromatography (HDC)

separation mode (the definition and applicability of HDC for polysaccharide separations will be discussed later). An example of these uncertainties introduced by calibration extrapolation for larger sizes in the analysis of starches is presented in Fig. 4. Four different extrapolation procedures for the calibration curve are compared (Fig. 4A): two linear calibration models (one for the region of SEC separation mode at lower V_h, model *'linear 1'*, and the other for the larger V_h region with HDC separation mode, model *'linear 2'*), and two polynomial calibration models (3rd and 5th order polynomials, respectively). The four different extrapolation procedures were applied separately to evaluate $\bar{M}_W(V_h)$ and $\bar{M}_n(V_h)$ through hydrodynamic volumes using MALLS, DRI and viscometric detection for commercial rice starch (Fig 4B). Large discrepancies at higher R_h are seen between the extrapolation procedures, leading to anomalous distributions. Indeed, higher apparent values of $\bar{M}_n(V_h)$ compared to those of $\bar{M}_W(V_h)$ are consistently obtained for the *linear 2* and both polynomial calibration models in the region beyond calibration; this is of course an artefact, since the dispersity $Đ(V_h) = \bar{M}_n(V_h)/\bar{M}_n(V_h)$ can never be less than 1. The values of $\bar{M}_W(V_h)$ are absolute and calculated directly from the MALLS and DRI signals independently from the calibration procedure; $\bar{M}_W(V_h)$ values are, on the other hand, calculated from Eq. (6) and therefore dependent on V_h, and very sensitive to the extrapolation procedure employed. It is essential to be aware that this calibration problem is only for amylopectin; the size range where reliable calibration can be performed includes amylose and glycogen.

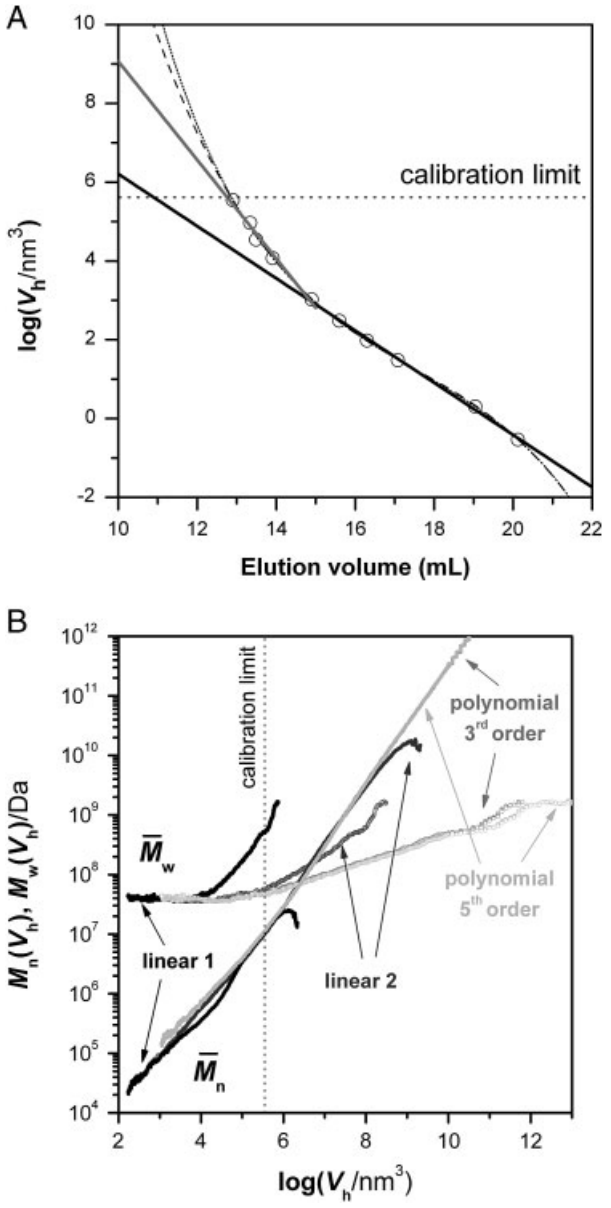

Figure 4. Uncertainties introduced by the extrapolation of the SEC calibration curves in the size regions where no standards are available. (A) Extrapolation of the calibration curves using four different mathematical procedures: linear 1 (black solid line, lower V_h region in the SEC separation mode), linear 2 (grey solid line, higher V_h region in the HDC separation mode), 3rd order polynomial (dashed line) and 5th order polynomial (dotted line). (B) $\bar{M}_W(V_h)$ and $\bar{M}_n(V_h)$ distributions for commercial rice starch (Sigma-Aldrich) obtained from SEC separation in DMSO/LiBr (0.5% w/w) coupled with triple detection (DRI, viscometric and MALLS), using extrapolation of the calibration curve with the four mathematical models: linear 1 (black), linear 2 (dark grey), 3rd order polynomial (grey) and 5th order polynomial (light grey).

A way to avoid the size calibration problem for larger macromolecular sizes is the use of light scattering calibration, *i.e.* using MALLS detection to obtain the relationship between elution volume and the radius of gyration, $\tilde{V}_{el}(R_g)$, and use the R_g so obtained as a complementary axis to R_h from universal calibration. In principle, this procedure has potential, since MALLS is especially sensitive to larger sizes and will offer enhanced sensitivity in this size range, where no standards for universal calibration are available. However, other considerations must be taken into account when implementing this procedure. The separation resolution with SEC for the larger sizes is not optimized, so poor separation and band-broadening issues may bias the calculated $\bar{R}_g$ values from light scattering. Moreover, the relationship between R_h (from universal calibration) and R_g is not well established for complex branched polymers and may depend on variables such as MW, dispersity, branching degree and macromolecular architecture. Indeed, the dependence between R_g and $R_{h,qels}$ (through the structural ratio $\rho = R_g/R_{h,qels}$, where the hydrodynamic radius $R_{h,qels}$ is that obtained by quasi-elastic light scattering (QELS)) shows strong deviations from theory for complex high-dispersity branched polysaccharides, such as glycogens and amylopectins [38]. Figure 5 displays the SEC weight distribution, $w(\log V_h)$, for commercial rice starch, plotted *versus* R_h (from universal calibration) in the lower *x*-axis and *versus* R_g (from light scattering calibration) in the upper *x*-axis. Comparable distributions are obtained using both calibration procedures for the amylose region, which is within the limits of the standards used here for universal calibration. Light scattering calibration offers in principle a more reliable size distribution for the amylopectin region, where

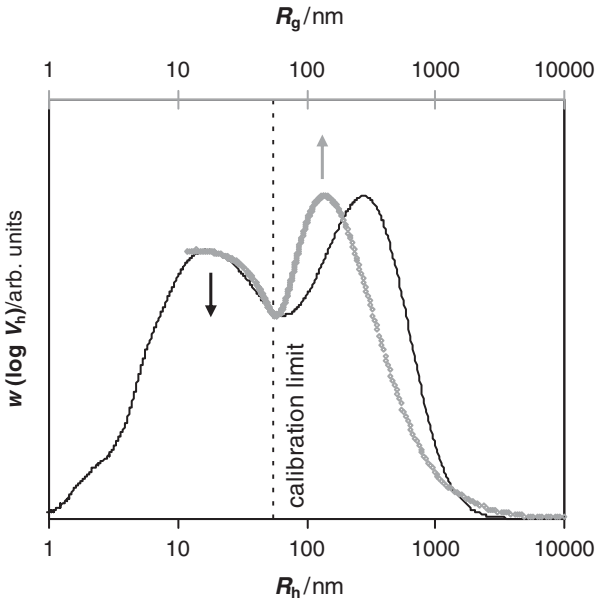

Figure 5. SEC weight distribution, $w(\log V_h)$, for commercial rice starch (Sigma-Aldrich) after SEC separation in DMSO/LiBr (0.5% w/w), plotted *versus* R_h (from universal calibration) in the lower *x*-axis and *versus* R_g (from light scattering calibration) in the upper *x*-axis.

extrapolation errors from universal calibration may alter the size distributions; insufficient light scattering signal for the smaller sizes, on the other hand, does not allow one to obtain the size distributions as a function of R_g for the smaller sizes. Extrapolation of a calibration curve is inaccurate for higher R_h, while the reverse holds for R_g from light scattering. Because there is some overlap between the regions where both are reliable, the combination should provide acceptable values for the size dependence of structural information over a wide range. The use of both size parameters to plot the resulting experimental distributions should be therefore used to overcome the experimental uncertainties and provide reliable structural information. Again, the size range where shear scission is a problem is that of amylopectin; amylose and glycogen, being much smaller, do not suffer from significant shear scission in SEC.

4.2.1.2 Band broadening

Band broadening is an instrumental limitation of all chromatographic separation techniques that results from longitudinal and axial dispersion during elution; this effect is distinct from the limitations of resolution and of peak capacity. This effect introduces an experimental error, in which species with the same size (*e.g.* hydrodynamic volume) that should co-elute at the same elution volume in practice elute over a certain range of volumes. Although modern SEC instrument and column technology minimizes this effect, it cannot be fully avoided during separation and must be taken into account when discussing experimental results. Methods for correcting band broadening through deconvolution using broad standards have been proposed (*e.g.* [49, 52–55]), but they have not yet been implemented in commercial SEC data manipulation software. For a full description of the chromatographic and sample-related aspects that affect band broadening and their effect on obtaining reliable size distributions of polydisperse polymers, the review from Popovici *et al.* is recommended [56].

Band broadening is expected to be particularly significant for the size range beyond the pore exclusion limit (this is, the range where HDC separation mode is predominant). This has implications for the separation of complex branched polysaccharides such as starch, since amylopectin populations often lie beyond the size ranges in which SEC columns offer optimal separations. The poor separation of amylopectin macromolecules and their co-elution in the size ranges of amylose (that lie in fact in the size range within the SEC separation mode and where band broadening should be minimized) may bias the resulting size distributions for starch. This effect will be particularly noticeable with MALLS detection, *i.e.* the $\bar{M}_W(V_h)$ and $\bar{R}_g(V_h)$ distributions, since light scattering is sensitive to MW, where there are large amylopectin molecules co-eluting with smaller amylose populations, they may mask and bias the corresponding detected $\bar{M}_W$ and $\bar{R}_g$ data. This can explain the anomalous results of the $\bar{M}_W(V_h)$ and $\bar{R}_g(V_h)$ distributions in the amylose region for rice starch seen in Fig. 6, where the apparent $\bar{M}_W$ and $\bar{R}_g$ values are higher than expected for amylose, which usually are in the range of 10^5–10^6 Da and 10–50 nm, respectively. The different contributions of the amylose and amylopectin populations to the light scattering behaviour have been pointed out previously [57]. Chemical fractionation of amylopectin and

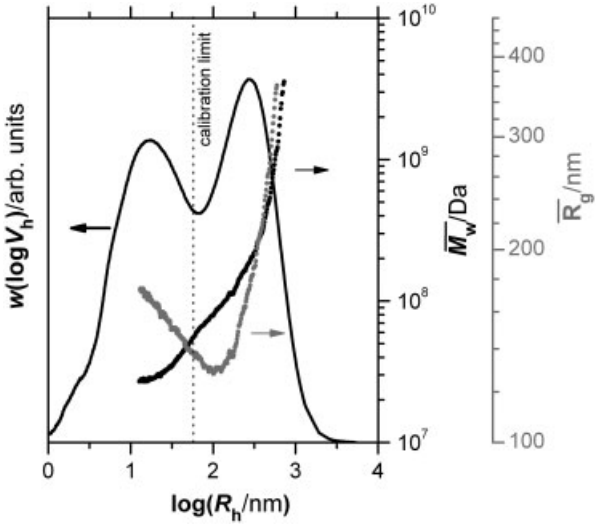

Figure 6. Showing of the uncertainties introduced by band broadening in the $\bar{M}_W(V_h)$ and $\bar{R}_g(V_h)$ distributions for commercial rice starch (Sigma-Aldrich) after SEC separation in DMSO/LiBr (0.5% w/w).

amylose may help to evaluate and avoid these undesired co-eluting effects on the size distributions of native starch; however, these wet-chemistry procedures are often tedious, time-consuming, incomplete and may lead to sample losses.

4.2.1.3 Shear scission

The occurrence of degradation through shear scission of high MW polymers during elution through SEC columns has been known for many years, but few studies have been made to elucidate the mechanisms of such a process [58, 59]. Such degradation phenomena can occur both in the interstitial medium and at the pore boundary, as well as in external 'plumbing' such as seals, with different mechanisms in each case, depending on the size of the eluting macromolecule [59]. Recent studies [60] on shear scission of branched polysaccharides (*e.g.* starch) during SEC and its analogy with droplet shear suggested that for low flow rates, medium-sized polysaccharides (including amylose, glycogen and other non-starch polysaccharides such as arabinoxylans and -glucans) are not substantially affected by shear scission. This inference was made using the quantitative analogy to droplet scission, which (as is well known in chemical engineering) can be analysed using an appropriate dimensionless number – the capillary number. This enables inferences to be made for the prevalence of shear scission for different sizes, viscosities and flow rates. This analysis also strongly suggests that, for the larger amylopectin macromolecules, there are no theoretical flow-rate conditions in which shear scission can be avoided with current technology. Indeed [60], alterations in the apparent size distributions for the amylopectin region are observed with different flow rates during SEC elution, indicating different extents of shear scission during separation. While this study used only a single set of columns, the flow-rate study, coupled with the dimensionless analysis of the phenomenon, indicated that SEC-induced scission of amylopectin could only be avoided with an improvement of about two orders of magnitude in appropriate conditions (*e.g.* using an eluent with a viscosity $\sim 10^{-2}$ cP = 1 mPa/s, which is impossible); this is such a large leap from the conditions of that study that it is unlikely that incremental improvements, such as larger-pore columns, could attain scission-free conditions while still achieving good separation. That is not to say that size separation of amylopectin has not been attained by SEC (it has been!), but that this separation caused some shear scission of the analyte.

Although shear scission of amylopectin during SEC is probably unavoidable with current technology, or technical improvements that are likely in the short term, such analyses can still provide qualitative and semi-quantitative information about the structural features of this large branched polysaccharide. Shear scission is expected to be reproducible through temporally close SEC runs, so semi-quantitative information may still be extracted from sample comparison. Moreover, recently 2-D structural distributions for native starch based on size and branching [61] show that the branching structure of amylopectin is independent of macromolecular size (see Section 4.3 of this review). The sheared amylopectin molecules are thus expected to maintain their branching structure even if shear scission occurs, since the mechanism of shear scission of amylopectin is most likely to occur in the centre of the molecule and thus give two moieties with similar sizes [62]. This inference (which has also been seen in starch extrusion [63]) is because the large torque needed to break a chemical bond mechanically depends on the centres of the two moieties that will be sheared being well spatially separated (torque being proportional to distance for a given velocity gradient), and the shear force on a very small moiety is much less than on a larger one. Improved separation technologies are required to obtain the full size distributions of native starch without shear degradation in solvent systems that fully dissolve starch. Unfortunately, up to this point there have been no published data in this regard.

4.2.1.4 Labelling of polysaccharides in SEC separations

Size separations of branched polysaccharides are to some extent hindered by the low sensitivity of the DRI concentration detector, due to the low values of dn/dc of such macromolecules in the common solvents employed for their separation. Labelling with chromophore or fluorophore enhances detection limits due to the high sensitivity of UV and fluorescence detectors. Such labelling could for example be on the single reducing end in a starch molecule, or elsewhere on the monomer unit throughout the molecule. There are some requirements, however, that the labelling procedure must meet, in order to be applicable for obtaining reliable size distributions for branched polysaccharides. Labelling must be either quantitative (that is, stoichiometrically performed in each of the polysaccharide molecules) or completely random (that is, performed in a representative ratio of the polysaccharide population, independent of molecular size, substitution, branching pattern and macromolecular architecture). If these requisites were followed, the resulting SEC analyses with UV or fluorescence detection would be able to offer reliable number and/or weight distributions for the labelled polysaccharides. Some approaches to labelling of starch-based polysaccharides and subsequent SEC analysis have been performed [64–67], but with the sole exception of the fluorophore labelling of the reducing end used in FACE, there has been no proof in any of these studies that these requirements have been satisfied.

4.2.1.5 Using size distributions of polysaccharides to unveil biological system

Two examples of the applicability of the size distributions from SEC separations and multiple detectors, to understand the biological function of branched polysaccharides are now

discussed for the case of arabinoxylan and glycogen. These polysaccharides have different macromolecular architectures (arabinoxylan is a copolymer with the monosaccharide monomer units attached to a linear backbone, whereas glycogen is a hyperbranched polysaccharide) but with similar sizes. These sizes fall within the range of both the calibration limits of SEC, and where the effect of shear scission on their structure is minimized.

Arabinoxylan is a substituted non-starch polysaccharide that has been reported to have beneficial effects in human diet, by increasing microbial fermentation and promoting beneficial microflora, preventing the absorption of bile acids, and retarding starch digestion. These beneficial nutritional effects are usually linked to viscosity and/or diffusion phenomena in the gastro-intestinal tract, which depend on arabinoxylan molecular structure [37]. Arabinoxylan is not a completely linear polysaccharide: it has α-L-arabinofuranose substituents attached to the (1–4)-β-D-xylopyranosyl linear backbone. Different size distributions, $w(\log V_h)$, $N(V_h)$, $\bar{M}_n(V_h)$, $\bar{M}_W(V_h)$ and $\bar{R}_g(V_h)$ were obtained [37] by SEC separation and multiple detection (DRI, viscometry, and MALLS) for three different arabinoxylans from different plant sources and different viscosities (Fig. 7); these distributions were used to understand anomalous behaviour found in the viscosity and diffusivity data. The size distributions and fractal dimensions were related to differences in the substitution pattern between the studied arabinoxylan samples, which significantly affect their capacity for supramolecular aggregation and therefore their viscosity and diffusivity.

Glycogen, which like starch is a hyperbranched glucose polymer with α-1,4 and α-1,6 links, has a structure similar to that of amylopectin, inasmuch as it has similar short-chain branches. There are the important differences: glycogen is randomly branched on a short distance scale, and has a relatively low MW (approximately 10^6 Da); it is thus unable to form crystalline structures. Native liver glycogen molecules arrange themselves in so-called β particles, which in turn form supramolecular structures called α particles. Comparison of experimental size distributions for undegraded native glycogen from rat liver (obtained using SEC separations with multiple detection) with the theoretical size distributions derived from the 'random branching model' [68, 69] reveals two distinct size regions in the distributions: one assigned to β particles formed by the random assembly of short branches, and another resulting from the random coupling of branched structures (β particles) into α particles [70]. These results, together with the fact that the average particle size does not decrease with the addition of high amounts of a hydrogen-bond disrupter (LiBr) to a solution in DMSO, suggest the existence of an unsuspected enzymatic process that covalently links β particles to form particles. Figure 8 shows the experimental size dependence of $\bar{M}_W(V_h)$, together with random-branching fitting to these data for the two distinct regions corresponding to α and β particles.

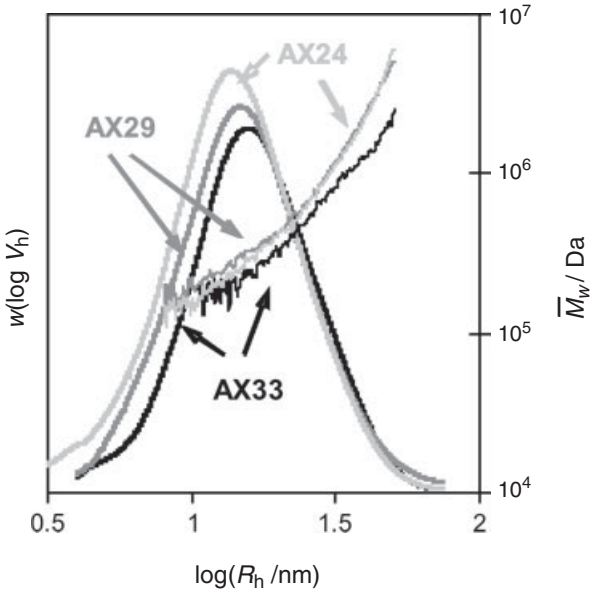

Figure 7. SEC distributions, $w(\log V_h)$ and (V_h) in terms of hydrodynamic radius, for three arabinoxylans samples with different viscosities (AX24, AX29 and AX33) in DMSO containing 0.5 wt% LiBr. Replotted from the data from Shelat *et al.* [37].

4.2.2 FFF

FFF technologies have attracted interest in the recent years for the separation of ultra-high MW macromolecules and particles. Separation is carried out by the application of an external field perpendicular to the sample elution flow, which causes the macromolecules to equilibrate according to an appropriate diffusion coefficient; separation then occurs along the developed laminar parabolic flow profile, where molecules elute in different linear velocity flow zones. Different external field forces can be applied, which has led to different FFF separation modes: a perpendicular cross-flow (symmetric- or asymmetric-field FFF, or AF^4), a thermal gradient (thermal FFF, ThFFF), centrifugal forces (sedimentation FFF, SdFFF), gravitational forces (gravita-

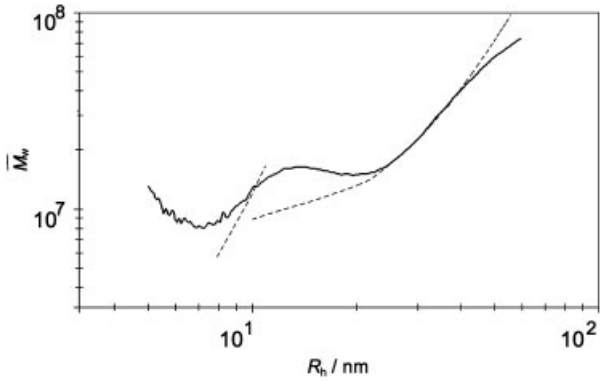

Figure 8. Dependence of MW on size, processed from the data in [70]. Full line: experiment; broken lines: fit to random branching model for α and β particles.

tional FFF, GrFFF), *etc*. Various reviews give a detailed overview about the theory and state-of-the-art of FFF technologies [71–73]. One of the main advantages of FFF techniques is that separation takes place in a channel without a stationary phase, so shear scission of the larger ultra-high MW molecules should be minimal.

FFF technologies have been successfully applied for the separation and structural analysis of commercial, partially degraded and/or modified polysaccharides, by coupling DRI and MALLS detection; this procedure allows one in principle to obtain the weight-average MW, $\bar{M}_W(V_{el})$, and the radius of gyration, $\bar{R}_g(V_{el})$ along the elution profile. Coupling of viscometric detection to FFF (which would give number distributions) is more complicated, even in principle, due to the sensitivity of this detector to pressure changes caused by the variable flow profiles during FFF. Size calibration of the elution volume is possible using the theory developed for each type of FFF technology, by relating the retention parameter λ to the corresponding diffusion coefficient (mass or thermal) D; a hydrodynamic diameter d_h can be thus calculated from the diffusion coefficient using the Stokes–Einstein relation (see References [74–76] for a full description of the theoretical development). However, these theoretical models make various approximations, and the complex experimental field profiles may introduce deviations from theory in the elution regime with respect to size calibration; thus the separation parameter is uncertain, which makes use of the resulting distributions questionable for (bio)synthesis–structure–property relations. Other calibration procedures may be performed, such as the injection of suitable standards and particles with monodisperse sizes or by using the radius of gyration $\bar{R}_g$ from MALLS as a size scale for elution volume calibration, which would enable the determination of reliable size distributions from FFF coupled with multiple detectors.

Application of asymmetric-flow FFF (AF^4) for structural characterization of polysaccharides has been reported for pullulan and dextran standards [77], cellulose derivatives [78–81], gum arabic (a highly branched arabinogalactan polysaccharide) [82], glycogen [83] and modified, degraded, commercial starch-based polysaccharides [83–89]. Sedimentation FFF (SdFFF) has been used to monitor the enzymatic degradation of starch granules [90] and for the investigation of the $\bar{M}_W$ and $\bar{R}_g$ distributions of destructured potato and waxy corn starches [91, 92]. Early studies reported the suitability of thermal FFF (ThFFF) for the separation of a wide range of polysaccharides, including pullulans, dextrans, starches and cellulose, in DMSO [93]; however, the difficulty of such separations for branched polysaccharides due to their poor solubility has also been pointed out.

In principle, AF^4 separation coupled with DRI and MALLS has potential advantages over other size-separation techniques such as SEC to reveal the full MW size distribution for undegraded native starch, since it avoids degradation of the large amylopectin molecules due to the absence of a stationary phase. As pointed out earlier, AF^4 has been already applied for the separation and structural characterization of starch-based polysaccharides, but these studies were either performed on chemically modified or degraded starches (with enhanced solubility in common solvents), or using sample preparation procedures and solvent systems that do not fully dissolve and/or degrade the original starch macromolecular structure. *Up to this point, no validated results are available on the size distributions of fully dissolved, undegraded native starch using FFF techniques.* In using AF^4 for size separation, it is essential to ensure that separation is by size (the Brownian elution mode), and not by some other, unknown separation parameter: *e.g.* the steric/hyperlayer mode (as has been reported for amylopectin [84]). The utilization of solvent systems that are known to fully dissolve starch macromolecules without the formation of aggregates (*e.g.* polar organic solvents with hydrogen-bond disrupting salts, such as DMSO with LiBr) may cause the deterioration of the AF^4 membranes. The low sensitivity of the concentration detectors employed for polysaccharides in their solvent systems (commonly, DRI detectors) is a limiting obstacle, since the large dilution of the injected polysaccharides during separation hinders obtaining concentration profiles with adequate resolution, and therefore prevents the calculation of accurate $\bar{M}_W$ values from MALLS. Indeed, under conditions where Brownian separation is achieved in a solvent system, which ensures complete dissolution (*e.g.* DMSO), the amylopectin concentration in the detector volume after elution is so low that the S/N is most unfavorable, and useful concentration data cannot be obtained. That means that one cannot obtain either $N(V_h)$ or $w(\log V_h)$ of native starches with current technology using AF^4. Overloading the channel is a major problem in these separations, since large amylopectin molecules may have the tendency to form aggregates and cause anomalous elution behaviour (steric elution mode) during each step of the separation process. Aggregate formation (which is likely if one were to attempt sufficiently high concentration to avoid the signal/noise problem with DRI detection) will give erroneous $\bar{M}_W$ and $\bar{R}_g$ readings after DRI and MALLS detection, which would be related to the aggregate but not to the fully dissolved macromolecular populations. Significant further development of AF^4 technology must be carried out to overcome the limitations that prevent the separation and full characterization of the size distributions of native amylopectin macromolecules.

4.2.3 HDC

HDC is in many ways similar to SEC. Separation takes place within a packed stationary phase with particles or within an open tubular system. The difference from SEC is that the particles do not contain pores, so the separation mechanism is slightly different and caused by the different solvent velocity profiles with respect of the surface of the stationary particles or the channel walls. Large molecules will be sterically excluded from the walls and will elute faster than smaller molecules, which can come closer to the wall

regions with slower velocity profiles. In HDC, the ratio between macromolecular size and the inter-particular diameter determines the efficiency of the separation. The theory of HDC and its application to polymer and particle separations have been well known for many years [94]; however, its wide implementation to polymer separation has been hindered to some extent by the popularity of SEC. In principle, coupling to the same detector systems as SEC is possible, and thus one would obtain similar size distributions through appropriate calibration procedures.

The applicability of HDC to branched polysaccharide size separation could be extended in the future to overcome the disadvantages of SEC, such as shear scission of the large ultra-high MW populations and calibration issues. Some preliminary attempts for starch size separations using HDC in a mixed-bed particle column and temperature gradients in aqueous mobile phases have been reported [95]. However, further technical developments are needed to optimize the stationary phase morphology to the range of macromolecular sizes to be separated and to guarantee their chemical stability with respect to the nature of solvents employed for full dissolution of the complex-branched polysaccharides.

4.2.4 Molecular-topology fractionation (MTF)

The separation of substituted and branched polysaccharides based on their branching degree or molecular architecture would enable a completely new means for structural characterization of such polymers and reveal new features about their (bio)synthesis and properties. Some attempts in this direction have recently been proposed for synthetic polymers with different topologies; separation of star polystyrenes with different number of branches has been achieved by MTF [96–98]. In this new mode of chromatography, separation of macromolecules based on their topology is achieved by elution in narrow channels at low flow rates. Under MTF conditions, separation occurs based on both size and topology. Below a critical size, separation by size is the predominant phenomenon; above the critical hydrodynamic volume, on the other hand, separation based on molecular topology occurs, where molecules with increased branching structure will be retained longer in the stationary phase. This critical size strongly depends on the morphology of the stationary phase.

The applicability of this new chromatographic separation mode to polysaccharides has not yet been reported, but it constitutes a promising area of research, especially for the separation of linear and branched amylose populations and the separation of modified polysaccharides based on their substitution pattern. New column technologies should be developed for these new applications, with suitable chemistries adapted for polysaccharide separations and optimized permeability and chemical resistance toward the polar solvents usually employed for polysaccharide analysis (*e.g.* DMSO with LiBr).

4.2.5 Temperature-gradient interaction chromatography (TGIC)

TGIC is a form of isocratic liquid interaction chromatography, where the temperature of the column is modified in a controlled way to promote the separation of macromolecules by MW by their enthalpic interaction with the stationary phase [99, 100]. Since TGIC is performed under isocratic conditions, it allows the use of a wide range of detectors (including differential refractometer and light scattering), which constitutes an advantage over other interaction-chromatography modes that use solvent gradients to promote the separation. TGIC can separate branched synthetic polymers with similar hydrodynamic volumes but different MWs with better resolution than SEC, as has been reported for macromolecules with different architectures such as star polystyrenes [101], styrene comb polymers [102], model dumbbell polymers [103] and hyperbranched polystyrenes (in combination with MALDI-TOF MS) [104, 105].

As far as we are aware, TGIC has not been applied yet to the separation of branched polysaccharides. Suitable conditions in terms of stationary phases, mobile phases and temperature gradients should be identified for each application, with the inconvenience that polysaccharides are susceptible to thermal degradation, which may reduce the range of temperatures that can be applied. However, the combination of SEC and TGIC could offer enhanced separation resolution, since both techniques have different separation mechanisms. In all such separations, it is not enough to have branch-sensitive separation, but one must also have some knowledge of what the separation parameter actually is, or at least a means of measuring this parameter after separation; this question does not appear to have yet been addressed.

4.2.6 Multidimensional separation and distributions

Multidimensional chromatographic separations offer in principle considerable potential for the separation of complex polysaccharides. Online coupling of interaction LC and SEC (LCxSEC) has been developed over the last few years for the separation of complex synthetic copolymers based on their size and chemical composition [106–110]. The implementation of such 2-D technologies could be of great utility for the high-resolution separation of substituted polysaccharides or polysaccharide derivatives with different chemical substitution pattern. However, solvent gradient LCxSEC set-ups may not be applicable for the separation of branched polysaccharides with complex architectures such as glycogen or starches, due to the absence of substantial chemical differences in their monomeric composition. Other modes, such as MTFxSEC or TGICxSEC, should be explored in these cases, once the topologic separation of branched polysaccharides is implemented. Coupling of multiple detectors could in all these hypothetical cases be performed after SEC in the second dimension, so multidimensional size distributions could be obtained after

separation. A coupling of MALLS detection after 2-D SECxSEC separation has been successfully implemented for synthetic polymers; implementation of such set-ups for polysaccharides with broad dispersity could enhance size-separation resolution and give more detailed size distributions [111].

The experimental implementation of multidimensional structural distributions for branched polysaccharides is deduced from the general theoretical description of the structure of branched polymers as an infinite-dimensional distribution based on the size and number of individual branches and their positions in the macromolecules [6]. Current characterization procedures by size-separation techniques and multiple detection (DRI, viscometer and light scattering detectors) give only 1-D projections of this multidimensional distribution. An analytical methodology to obtain the experimental 2-D distribution for branched polysaccharides (native starch), based on size and branching has been recently implemented [61], as the two structural dimensions describing the total macromolecular size (V_h) and the DP of a branch in that molecule. The analytical procedure uses the fact that starch can be quantitatively debranched using enzymatic treatment and is implemented by performing off-line 2-D SEC) on the branched whole molecules and on their debranched counterparts. The first step uses preparative SEC to obtain a number of fractions from the original native starch sample with sufficient size resolution (V_h, the first dimension). Different size distributions of the collected fractions, both before and after debranching, are obtained using analytical SEC coupled with triple detection (DRI, viscometry and MALLS); the SEC set-ups for the analysis of the whole branched and linear debranched starch populations were optimized to enhance resolution and minimize the effects of shear scission [60]. The result is the first 2-D distribution for starch: the weight SEC distribution $w(\log(\bar{R}_h, \bar{X}_{de}))$ based on macromolecular size $\bar{R}_h$ as the first dimension and chain-length distribution of the branches $\bar{X}_{de}$ as the second dimension (Fig. 9). $\bar{R}_h$ and $\bar{X}_{de}$ are averages because of imperfect separation (band broadening) in the fractionation step. This distribution reveals new structural features in native starch macromolecules, the well-known amylopectin and amylose populations, and also hybrid macromolecular populations [61]. The results give new insights into the underlying biosynthetic processes. This analytical procedure could in principle be implemented to any branched or substituted polysaccharide or synthetic polymer in which quantitative debranching is possible. The potential of this new method for revealing (bio)synthesis–structure–property relations in complex polysaccharides remains to be fully explored.

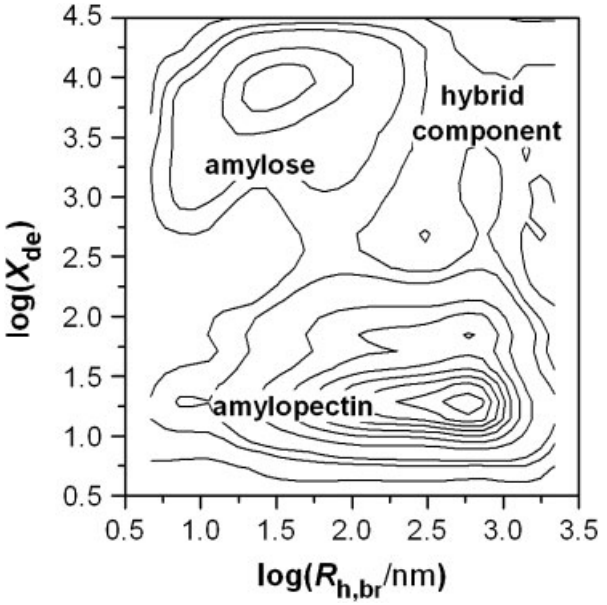

Figure 9. Contour plot of the 2-D experimental SEC weight distribution $w(\log(\bar{R}_h, \bar{X}_{de}))$ for native rice starch based on macromolecular size and branch chain-length. Replotted using experimental data from [61].

5 Concluding remarks and future directions

Structural characterization using different size-separation techniques and a number of detectors (number-, concentration- and MW-sensitive) provides valuable information about several structural levels in substituted/branched polysaccharides, namely the branch chain-length distribution and the branched macromolecular architecture. These size distributions constitute the experimental core with which to elucidate the (bio)synthesis–structure–property relations of such polysaccharides, of fundamental importance in biological systems and with health, nutrition and industrial applications. The development of sample preparation methods that (i) ensure complete dissolution of the target polysaccharides in the solvent systems employed for size separation, (ii) minimize degradation, aggregation and other undesirable effects and (iii) eliminate possible contaminants that may overshadow important structural features of the analytes, is an essential preliminary to obtaining reliable experimental distributions.

FACE constitutes the method of choice to analyse the chain-length distribution of the branches with DP up to ~85, with individual peak resolution; SEC must be used for bigger branches, although there are problems with band broadening. The full structural analysis of the whole branched polysaccharide constitutes a major challenge, since there are no methods that provide meaningful size distributions of such complex macromolecules over the entire size range of interest. SEC represents the technique of choice for such separations, in spite of the well-known problems of calibration, band broadening and shear scission of the larger macromolecules. These issues have been addressed and discussed in the present review, especially for the case of starch macromolecules. However, SEC coupled with multiple detection is a robust and well-developed technology, which provides reliable size distributions for

medium-sized polysaccharides (two examples have been discussed here for glycogen and arabinoxylans). FFF technologies have potential to overcome the limitations of SEC for larger and more complex-branched polysaccharides. Some progress has been made for the separation and structural characterization of commercial, partially degraded and/or modified polysaccharides using asymmetric-flow FFF (AF^4). However, up to this point, obtaining size distributions of fully dissolved undegraded native starch has not been achieved using FFF separation, due to technical problems associated with the nature of such separation technologies and the complex structure of starch (aggregation problems, low resolution of the concentration detectors, complex flow profiles in the solvent systems that achieve full dissolution of the polysaccharides, *etc.*). Significant technical development in separation technology is needed to achieve reliable size distributions of the most complex-branched polysaccharides (*e.g.* native amylopectin in starch). New separation technologies that are sensitive to branching structure (*e.g.* MTF) may be very useful to cast some light on structural features of these macromolecules. 2-D separations should be explored, and those obtained in the first studies show how this additional information can shed new light on biosynthetic processes. All these challenges are motivation to develop improved separation procedures with enhanced detector sensitivity, which will allow obtaining reliable size distributions for complex-branched polysaccharides.

The support of the Australian Research Council (grants DP0985694 and DP0986043) is gratefully acknowledged. F. V. gratefully acknowledges the support of the Knut and Alice Wallenberg Foundation (Sweden) for a postdoctoral fellowship. Dr. Jovin Hasjim is thanked for valuable discussions and comments.

The authors have declared no conflict of interest.

6 References

[1] Sinnott, M., *Carbohydrate Chemistry and Biochemistry: Structure and Mechanism*, The Royal Society of Chemistry, Cambridge, UK 2007.

[2] Mischnick, P., *Cellulose* 2001, *8*, 245–257.

[3] McIntyre, D. D., Ho, C., Vogel, H. J., *Starch-Staerke* 1990, *42*, 260–267.

[4] Richardson, S., Gorton, L., *Anal. Chim. Acta* 2003, *497*, 27–65.

[5] Mischnick, P., Heinrich, J., Gohdes, M., Wilke, O., Rogmann, N., *Macromol. Chem. Phys.* 2000, *201*, 1985–1995.

[6] Gray-Weale, A., Gilbert, R. G., *J. Polym. Sci. Part A Polym. Chem. Ed.* 2009, *47*, 3914–3930.

[7] Gidley, M. J., Hanashiro, I., Hani, N. M., Hill, S. E., Huber, A., Jane, J.-L., Liu, Q., Morris, G. A., Rolland-Sabaté, A., Striegel, A., Gilbert, R. G., *Carbohydr. Polym.* 2010, *79*, 255–261.

[8] Bello-Pérez, L. A., Roger, P., Baud, B., Colonna, P., *J. Cereal Sci.* 1998, *27*, 267–278.

[9] Han, J.-A., Lim, S.-T., *Carbohydr. Polym.* 2004, *55*, 265–272.

[10] Kim, H.-S., Huber, K. C., Higley, J. S., *J. Agric. Food Chem.* 2006, *54*, 9664–9669.

[11] You, S., Lim, S.-T., *Cereal Chem.* 2000, *77*, 303–308.

[12] Syahariza, Z. A., Li, E., Hasjim, J., *Carbohydr. Polym.* 2010, *82*, 14–20.

[13] Schmitz, S., Dona, A. C., Castignolles, P., Gilbert, R. G., Gaborieau, M., *Macromol. Biosci.* 2009, *9*, 506–514.

[14] Ryu, J.-H., Drain, J., Kim, J. H., McGee, S., Gray-Weale, A., Waddington, L., Parker, G. J., Hargreaves, M., Yoo, S.-H., Stapleton, D., *Int. J. Biol. Macromol.* 2009, *45*, 478–482.

[15] Jones, R. G., Kahovec, J., Stepto, R., Wilks, E. S., Hess, M., Kitayama, T., Metanomski, W. V., *Compendium of Polymer Terminology and Nomenclature. IUPAC Recommendations 2008*, Royal Society of Chemistry, Cambridge, UK 2009.

[16] Clay, P. A., Gilbert, R. G., *Macromolecules* 1995, *28*, 552–569.

[17] Gaborieau, M., Gilbert, R. G., Gray-Weale, A., Hernandez, J. M., Castignolles, P., *Macromol. Theory Simul.* 2007, *16*, 13–28.

[18] O'Shea, M. G., Samuel, M. S., Konik, C. M., Morell, M. K., *Carbohydr. Res.* 1998, *307*, 1–12.

[19] Hamielec, A. E., Ouano, A. C., *J. Liq. Chromatogr.* 1978, *1*, 111–120.

[20] Hamielec, A. E., Ouano, A. C., Nebenzahl, L. L., *J. Liq. Chromatogr.* 1978, *1*, 527–554.

[21] Kostanski, L. K., Keller, D. M., Hamielec, A. E., *J. Biochem. Biophys. Methods* 2004, *58*, 159–186.

[22] Zimm, B. H., *J. Chem. Phys.* 1948, *16*, 1093–1099.

[23] Wyatt, P. J., *Anal. Chim. Acta* 1993, *272*, 1–40.

[24] Berry, G. C., in: Pethrick, R. A., Stein, R. S. (Eds.), *Experimental Methods in Polymer Characterization*, Wiley, London, UK 1998.

[25] Burchard, W., in: Harding, S. E., Sattelle, D. B., Bloomfield, V. A. (Eds.), *Laser Light Scattering in Biochemistry*, Royal Society Chemistry, Cambridge, UK 1992, pp. 3–22.

[26] Burchard, W., *Adv. Polym. Sci.* 1983, *48*, 1–124.

[27] Zimm, B. H., *J. Chem. Phys.* 1948, *16*, 1099–1116.

[28] Debye, P., *J. Phys. Colloid Chem.* 1947, *51*, 18–32.

[29] Berry, G. C., *J. Chem. Phys.* 1966, *44*, 4550–4564.

[30] Andersson, M., Wittgren, B., Wahlund, K.-G., *Anal. Chem.* 2003, *75*, 4279–4291.

[31] Burchard, W., *Macromolecules* 1977, *10*, 919–927.

[32] Galinsky, G., Burchard, W., *Macromolecules* 1997, *30*, 4445–4453.

[33] Burchard, W., *Macromolecules* 1972, *5*, 604–610.

[34] Burchard, W., *Adv. Polym. Sci.* 1999, *143*, 113–194.

[35] de Gennes, P.-G., *Scaling Concepts in Polymer Physics*, Cornell University, Ithaca, NY 1979.

[36] Burchard, W., *Macromolecules* 2004, *37*, 3841–3849.

[37] Shelat, K. J., Vilaplana, F., Nicholson, T. M., Wong, K. H., Gidley, M. J., Gilbert, R. G., *Carbohydr. Polym.* 2010, *82*, 46–53.

[38] Rolland-Sabaté, A., Mendez-Montealvo, M. G., Colonna, P., Planchot, V., *Biomacromolecules* 2008, *9*, 1719–1730.

[39] Morell, M. K., Samuel, M. S., O'Shea, M. G., *Electrophoresis* 1998, *19*, 2603–2611.

[40] Kazarian, A. A., Breadmore, M. C., Hilder, E. F., in: Volpi, N. (Ed.), *Capillary Electrophoresis of Carbohydrates: From Monosaccharides to Complex Polysaccharides*, Humana Press, New York, NY 2010.

[41] Hanashiro, I., Abe, J., Hizukuri, S., *Carbohydr. Res.* 1996, *283*, 151–159.

[42] Wong, K. S., Jane, J., *J. Liq. Chromatogr.* 1995, *18*, 63–80.

[43] Koch, K., Andersson, R., Aman, P., *J. Chromatogr. A* 1998, *800*, 199–206.

[44] Broberg, S., Koch, K., Andersson, R., Kenne, L., *Carbohydr. Polym.* 2000, *43*, 285–289.

[45] Castro, J. V., Dumas, C., Chiou, H., Fitzgerald, M. A., Gilbert, R. G., *Biomacromolecules* 2005, *6*, 2248–2259.

[46] Cuevas, R. P., Daygon, D., Morell, M., Gilbert, R. G., Fitzgerald, M. A., *Carbohydr. Polym.* 2010, *81*, 120–127.

[47] Castro, J. V., Ward, R. M., Gilbert, R. G., Fitzgerald, M. A., *Biomacromolecules* 2005, *6*, 2260–2270.

[48] Castro, J. V., van Berkel, K. Y., Russell, G. T., Gilbert, R. G., *Aust. J. Chem.* 2005, *58*, 178–181.

[49] Konkolewicz, D., TaylorII, J. W., Castignolles, P., Gray-Weale, A. A., Gilbert, R. G., *Macromolecules* 2007, *40*, 3477–3487.

[50] Kilz, P., in: Wu, C.-s. (Ed.), *Column Handbook for SEC*, Academic Press, San Diego, CA 1999.

[51] Kuge, T., Kobayashi, K., Tanahashi, H., Igushi, T., Kitamura, S., *Agric. Biol. Chem.* 1984, *78*, 2375–2376.

[52] Schnöll-Bitai, I., *J. Chromatogr. A* 2005, *1084*, 160–166.

[53] Yossen, M. M., Vega, J. R., Meira, G. R., *J. Chromatogr. A* 2006, *1128*, 171–180.

[54] Gruendling, T., Guilhaus, M., Barner-Kowollik, C., *Anal. Chem.* 2008, *80*, 6915–6927.

[55] Meira, G., Netopilik, M., Potschka, M., Schnoll-Bitai, I., Vega, J., *Macromol. Symp.* 2007, *258*, 186–197.

[56] Popovici, S.-T., Kok, W. T., Schoenmakers, P. J., *J. Chromatogr. A* 2004, *1060*, 237–252.

[57] Roger, P., Bello-Perez, L. A., Colonna, P., *Polymer* 1999, *40*, 6897–6909.

[58] Barth, H. G., Carlin, F. J., *J. Liq. Chromatogr.* 1984, *7*, 1717–1738.

[59] Striegel, A. M., *J. Liq. Chromatogr. Relat. Technol.* 2008, *31*, 3105–3114.

[60] Cave, R. A., Seabrook, S. A., Gidley, M. J., Gilbert, R. G., *Biomacromolecules* 2009, *10*, 2245–2253.

[61] Vilaplana, F., Gilbert, R. G., *Macromolecules* 2010, *43*, DOI 10.1021/ma101349t.

[62] Basedow, A. M., Ebert, K. H., *Adv. Polym. Sci.* 1977, *22*, 83–148.

[63] Liu, W.-C., Halley, P. J., Gilbert, R. G., *Macromolecules* 2010, *43*, 2855–2864.

[64] Hoang, N.-L., Landolfi, A., Kravchuk, A., Girard, E., Peate, J., Hernandez, J. M., Gaborieau, M., Kravchuk, O., Gilbert, R. G., Guillaneuf, Y., Castignolles, P., *J. Chromatogr. A* 2008, *1205*, 60–70.

[65] Takeda, Y., Shibahara, S., Hanashiro, I., *Carbohydr. Res.* 2003, *338*, 471–475.

[66] Hanashiro, I., Takeda, Y., *Carbohydr. Res.* 1998, *306*, 421–426.

[67] Praznik, W., Huber, A., *J. Chromatogr. B Analyt. Technol. Biomed. Life Sci.* 2005, *824*, 295–307.

[68] Konkolewicz, D., Gilbert, R. G., Gray-Weale, A., *Phys. Rev. Lett.* 2007, *98*, 238301–238304.

[69] Konkolewicz, D., Thorn-Seshold, O., Gray-Weale, A., *J. Chem. Phys.* 2008, *19*, 054901.

[70] Sullivan, M. A., Vilaplana, F., Cave, R. A., Stapleton, D. I., Gray-Weale, A. A., Gilbert, R. G., *Biomacromolecules* 2010, *11*, 1094–1100.

[71] Roda, B., Zattoni, A., Reschiglian, P., Moon, M. H., Mirasoli, M., Michelini, E., Roda, A., *Anal. Chim. Acta* 2009, *635*, 132–143.

[72] Williams, S. K. R., Lee, D., *J. Sep. Sci.* 2006, *29*, 1720–1732.

[73] Messaud, F. A., Sanderson, R. D., Runyon, J. R., Otte, T., Pasch, H., Williams, S. K. R., *Prog. Polym. Sci.* 2009, *34*, 351–368.

[74] Schimpf, M., Cladwell, K., Giddings, J. C. (Eds.), *Field-Flow Fractionation Handbook*, Wiley-Interscience, New York, NY 2000.

[75] Giddings, J. C., Yang, F. J. F., Myers, M. N., *Science* 1976, *193*, 1244–1245.

[76] Giddings, J. C., Yang, F. J., Myers, M. N., *Anal. Chem.* 1976, *48*, 1126–1132.

[77] Wittgren, B., Wahlund, K.-G., *J. Chromatogr. A* 1997, *760*, 205–218.

[78] Wittgren, B., Wahlund, K. G., *Carbohydr. Polym.* 2000, *43*, 63–73.

[79] Porsch, B., Andersson, M., Wittgren, B., Wahlund, K.-G., *J. Chromatogr. A* 2002, *946*, 69–81.

[80] Andersson, M., Wittgren, B., Wahlund, K.-G., *Anal. Chem.* 2001, *73*, 4852–4861.

[81] Andersson, M., Wittgren, B., Schagerlof, H., Momcilovic, D., Wahlund, K.-G., *Biomacromolecules* 2003, *5*, 97–105.

[82] Picton, L., Bataille, I., Muller, G., *Carbohydr. Polym.* 2000, *42*, 23–31.

[83] Rolland-Sabate, A., Colonna, P., Mendez-Montealvo, M. G., Planchot, V., *Biomacromolecules* 2007, *8*, 2520–2532.

[84] van Bruijnsvoort, M., Wahlund, K. G., Nilsson, G., Kok, W. T., *J. Chromatogr. A* 2001, *925*, 171–182.

[85] Roger, P., Baud, B., Colonna, P., *J. Chromatography A* 2001, *917*, 179–185.

[86] Lee, S., Nilsson, P. O., Nilsson, G. S., Wahlund, K. G., *J. Chromatogr. A* 2003, *1011*, 111–123.

[87] Lee, S., Kim, S. T., Pant, B. R., Kwen, H. D., Song, H. H., Lee, S. K., Nehete, S. V., *J. Chromatogr. A* 2010, *1217*, 4623–4628.

[88] Rojas, C. C., Wahlund, K.-G., Bergenstahl, B., Nilsson, L., *Biomacromolecules* 2008, *9*, 1684–1690.

[89] You, S., Stevenson, S. G., Izydorczyk, M. S., Preston, K. R., *Cereal Chem.* 2002, *79*, 624–630.

[90] Morelon, X., Battu, S., Salesse, C., Begaud-Grimaud, G., Cledat, D., Cardot, P. J. P., *J. Chromatogr. A* 2005, *1093*, 147–155.

[91] Hanselmann, R., Burchard, W., Ehrat, M., Widmer, H. M., *Macromolecules* 1996, *29*, 3277–3282.

[92] Hanselmann, R., Ehrat, M., Widmer, H. M., *Starch-Starke* 1995, *47*, 345–349.

[93] Lou, J., Myers, M. N., Giddings, J. C., *J. Liq. Chromatogr.* 1994, *17*, 3239–3260.

[94] Stegeman, G., Kraak, J. C., Poppe, H., Tijssen, R., *J. Chromatogr. A* 1993, *657*, 283–303.

[95] Dias, R. P., Fernandes, C. S., Mota, M., Teixeira, J., Yelshin, A., *Carbohydr. Polym.* 2008, *74*, 852–857.

[96] Edam, R., Meunier, D. M., Mes, E. P. C., Van Damme, F. A., Schoenmakers, P. J., *J. Chromatogr. A* 2008, *1201*, 208–214.

[97] Meunier, D. M., Smith, P. B., Baker, S. A., *Macromolecules* 2005, *38*, 5313–5320.

[98] Meunier, D. M., Stokich, T. M., Gillespie, D., Smith, P. B., *Macromol. Symp.* 2007, *257*, 56–70.

[99] Chang, T., Lee, H. C., Lee, W., Park, S., Ko, C., *Macromol. Chem. Phys.* 1999, *200*, 2188–2204.

[100] Ryu, J., Chang, T., *Anal. Chem.* 2005, *77*, 6347–6352.

[101] Lee, H. C., Chang, T., Harville, S., Mays, J. W., *Macromolecules* 1998, *31*, 690–694.

[102] Chambon, P., Fernyhough, C. M., Im, K., Chang, T., Das, C., Embery, J., McLeish, T. C. B., Read, D. J., *Macromolecules* 2008, *41*, 5869–5875.

[103] Rajan, M., Velthem, P. V., Zhang, M., Cho, D., Chang, T., Agarwal, U. S., Bailly, C., George, K. E., Lemstra, P. J., *Macromolecules* 2007, *40*, 3080–3089.

[104] Im, K., Park, S., Cho, D., Chang, T., Lee, K., Choi, N., *Anal. Chem.* 2004, *76*, 2638–2642.

[105] Ryu, J., Im, K., Yu, W., Park, J., Chang, T., Lee, K., Choi, N., *Macromolecules* 2004, *37*, 8805–8807.

[106] Kilz, P., Kruger, R. P., Much, H., Schulz, G., *Adv. Chem. Ser.* 1995, *247*, 223–241.

[107] Adrian, J., Esser, E., Hellmann, G., Pasch, H., *Polymer* 2000, *41*, 2439–2449.

[108] van der Horst, A., Schoenmakers, P. J., *J. Chromatogr. A* 2003, *1000*, 693–709.

[109] Kilz, P., Pasch, H., *Coupled Liquid Chromatographic Techniques in Molecular Characterization*, Wiley New York 2006.

[110] Kilz, P., *Chromatographia* 2003, *59*, 3–14.

[111] Moyses, S., *J. Sep. Sci.* 2010, *33*, 1480–1486.

